The WIPE assay for selection and elimination of HIV-1 provirus *in vitro* using latency-reversing agents

Kouki Matsuda[1‡], Saiful Islam[2‡], Kiyoto Tsuchiya[3], Benjy Jek Yang Tan[2], Shin-ichiro Hattori[1], Hiroo Katsuya[2§], Paola Miyazato[2], Misaki Matsuo[2], Nicole S. Delino[1], Hiroyuki Gatanaga[3], Shinichi Oka[3], Kazuhisa Yoshimura[2,4,5], Shuzo Matsushita[2], Hiroaki Mitsuya[1,6], Yorifumi Satou[2‡*], and Kenji Maeda[1‡*]

[1]National Center for Global Health and Medicine Research Institute, Tokyo, Japan; [2]Joint Research Center for Human Retrovirus Infection, Kumamoto University, Kumamoto, Japan; [3]AIDS Clinical Center, National Center for Global Health and Medicine, Tokyo, Japan; [4]AIDS Research Center, National Institute of Infectious Diseases, Tokyo, Japan; [5]Tokyo Metropolitan Institute of Public Health, Tokyo, Japan; [6]HIV and AIDS Malignancy Branch, National Cancer Institute, National Institutes of Health, Maryland, USA.

[*] Address correspondence to Kenji Maeda, kmaeda@ri.ncgm.go.jp, or Yorifumi Satou, y-satou@kumamoto-u.ac.jp

[‡] Equal contribution

[§] Current affiliation: Division of Hematology, Respiratory Medicine, and Oncology, Department of Internal Medicine, Faculty of Medicine, Saga University

ABSTRACT

Persistence of HIV-1 latent reservoir cells during antiretroviral therapy (ART) is a major obstacle for curing HIV-1. Latency-reversing agents (LRAs) are under intensive development to reactivate and eradicate latently infected cells; however, there are a few useful models for evaluating LRA activity *in vitro*. Here, we established a chronically HIV-1-infected culture system harboring thousands of different HIV-1-infected cell clones with a wide distribution of HIV-1 provirus similar to that observed *in vivo*. A combination of an LRA and an anti-HIV-1 drug successfully inhibited viral re-emergence after drug discontinuation, demonstrating "experimental cure" in the *in vitro* model. We demonstrated that the epigenetic environment of the integrated provirus plays a role in determining drug susceptibility. Our widely distributed intact provirus elimination (WIPE) assay will be useful for optimizing therapeutics against HIV-1 latency and provides mechanistic insights into the selection of heterogeneous HIV-1-infected clones during drug treatment.

INTRODUCTION

Advances in antiviral therapy have dramatically improved the therapeutic options available for treating human immunodeficiency virus type 1 (HIV-1) infection. However, even with the most potent combined antiretroviral therapy (cART), HIV-1-infected patients remain on medication throughout their lifetime because HIV-1 persists in viral reservoirs *in vivo* regardless of treatment[1-3]. In this regard, the "shock and kill" approach, which first activates cells latently infected with HIV-1[2,3] using small molecule agents called HIV-1 latency-reversing agents (LRAs), is a possible strategy for curing HIV-1[4-9]. LRAs reverse HIV-1 latency and induce viral production in cells latently infected with the virus. In theory, infected cells that express viral antigens are then killed by the human immune system, such as cytotoxic T lymphocytes, or viral cytopathic effects[10-12]. However, LRAs that appear potent in *in vitro* assays are not necessarily effective *in vivo* because the viral reservoir situation is quite different *in vitro* and *in vivo*[13-16]. The host factors shaping the HIV-1 reservoir *in vivo* include the immunological status with respect to the virus, anatomical location, and a variety of host cells. From the viral perspective, wide heterogeneity is noted *in vivo*, such as the viral sequence, presence of defective proviruses, integration sites (ISs) in the host cellular genomic DNA, and expansion of some infected clones[17-21]. These factors potentially affect the efficacy of LRA *in vivo*.

As the "shock" step may trigger the production of infectious virus and thereby induce *de novo* infection, it is essential to combine LRAs with the existing anti-HIV-1 drugs. However, no suitable *in vitro* model system to evaluate the efficacy of such combination therapies exists. Currently available *in vitro* models for HIV-1 latency, such as ACH2, J1.1, and U1 cells, carry only one or two integrated proviruses with a specific genetic and epigenetic pattern, but there are thousands of different integration sites for HIV-1 *in vivo*. Therefore, LRAs can reactivate some HIV-1 proviruses in *in vitro* models, but that may not be the case for other HIV-1 proviruses integrated in a different host genome. According to a recent study, a combination of anti-HIV-1 drugs with an LRA (Toll-like receptor 7 agonist GS-9620) and a broadly

neutralizing anti-HIV-1 antibody (PGT121) successfully delays or inhibits viral rebound, following discontinuation of antiretroviral therapy in simian HIV-infected rhesus monkey[22]. Hence, *in vivo* animal models are useful for preclinical evaluation during drug development; however, the need for a specialized facility and the associated high experimental costs limit their availability for drug screening. *In vitro* systems capable of evaluating the combined effects of anti-HIV-1 drugs and LRAs are urgently required to enhance the development of LRAs.

In the present study, we aimed to establish a new *in vitro* infection model that harbors a much wider variety of HIV-1-infected clones than that of conventional *in vitro* models. Our *in vitro* model mimics the viral reservoir observed *in vivo* and is suitable for investigating not only possible drug combination(s) effective in eliminating HIV-1 reservoirs in the human body but also the mechanism by which HIV-1 latent cells are maintained in the reservoirs for prolonged periods of time.

RESULTS

Development of an *in vitro* model mimicking the distribution of HIV-1 provirus *in vivo*. To establish an HIV-1 chronically-infected *in vitro* model with a variety of HIV-1-infected clones, several host cell lines were infected with an HIV-1 infectious clone, HIV-1_{NL4-3} or HIV-1_{JRFL}. The cells were then cultured, and cell growth and HIV-1 level (production) in the supernatant monitored twice a week. MT-4 cells infected with HIV-1_{NL4-3} died rapidly and no live cells were observed after 30 d (data not shown). We analyzed intracellular p24 expression in samples with adequate cell viability on day 30. Jurkat cells infected with HIV-1_{NL4-3} (Jurkat/NL) maintained high levels of HIV-1 productivity (**Fig. 1a**) and intracellular HIV-1 DNA (**Fig. 1b**). PM1CCR5 cells infected with HIV-1_{JRFL} (PM1CCR5/JRFL) also maintained HIV-1 production and intracellular HIV-1 DNA levels after 30 d of culture; however, the p24 level in the supernatant decreased after 90 d (data not shown). Flow cytometry analyses on day 30 revealed four distinct cell populations, i.e., p24-negative live cells, p24-negative dead cells, p24-positive live cells,

and p24-positive dead cells (**Fig. 1c**), in the three tested infected cell lines. Based on these results, we focused on Jurkat/NL in the present study.

We confirmed the infectivity of viruses in the supernatant of Jurkat/NL cells using MT-4 cells (**Supplementary Fig. 1a**). We further investigated the number of HIV-1-infected clones in the *in vitro* culture model. In principle, each HIV-1-infected clone has a different viral IS, which can be used to distinguish clones. We performed ligation-mediated polymerase chain reaction (LM-PCR) to detect the junctions between the 3′-long terminal repeat (LTR) of HIV-1 and the flanking host genome sequence[23,24]. We used 500 ng of genomic DNA and detected approximately 1,000 different ISs, demonstrating the presence of thousands of different infected clones in the *in vitro* infection model (**Fig. 1d**). This was in stark contrast with ACH-2, J1.1, and U1 cell lines, in which only two ISs were detected[25] (**Fig. 1d**). Next, we tested whether the distribution of HIV-1 proviruses in the *in vitro* system was equivalent to that found *in vivo*. We analyzed HIV-1 ISs in peripheral blood mononuclear cells (PBMCs) isolated from HIV-1-infected individuals following the same protocol as that for *in vitro* cultured cells. We observed similarities between HIV-1 integration *in vivo* and *in vitro*, i.e., increased integration incidence in certain chromosomes (**Fig. 1e**). Furthermore, HIV-1 preferentially integrated into the gene-containing regions both *in vitro* and *in vivo*, compared with random distribution (**Fig. 1f**). These data indicate similarities of HIV-1 ISs between the newly developed *in vitro* infection model and *in vivo* patient material.

The novel *in vitro* infection model can be used to screen the effectiveness of LRA and anti-HIV-1 drug combinations. We next evaluated the efficacy of antiretroviral agents and/or LRAs against various HIV-1-infected clones in the *in vitro* culture system. We cultured Jurkat/NL cells in the presence or absence of an antiretroviral drug and/or a LRA (**Fig. 2a**). We used the antiretroviral drug EFdA (4′-ethynyl-2-fluoro-2′-deoxyadenosine)/MK-8591/islatravir (ISL), which is a potent nucleoside reverse-transcriptase inhibitor and currently under clinical

trials[26,27]. We evaluated 11 LRAs to determine their activity in Jurkat/NL cells, and found that PEP005 [ingenol-3-angelate, protein kinase C (PKC) activator][6] induced HIV-1 production and apoptosis in HIV-1-infected cells at the lowest concentration tested (**Supplementary Fig. 1b and c**). Furthermore, 1 μM SAHA and panobinostat induced strong caspase-3 activation (**Supplementary Fig. 1c**); however, the same concentration of these drugs also induced strong cell toxicity in HIV-1-negative cells (data not shown). Hence, we used PEP005 in subsequent experiments. Treatments with EFdA (50 nM), PEP005 (5 nM), or a combination of EFdA and PEP005 were started simultaneously, and supernatant p24 levels were monitored for 4 months (**Fig. 2a**). Cumulative data from multiple independent experiments are shown in **Fig. 2b.** Treatment with PEP005 alone did not suppress HIV-1 replication during the first 9 weeks of cultivation, while EFdA alone successfully decreased viral numbers in the supernatant to undetectable levels after 4–6 weeks. The combination treatment with EFdA and PEP005 also decreased the amount of HIV-1 in the supernatant to undetectable levels.

We next interrupted the drug treatment in week 9 and observed a remarkable rebound of viral production in samples treated with EFdA alone (11/11, 100%); however, no rebound was apparent in 64% (7/11) of samples treated with the combination of EFdA and PEP005 (**Fig. 2b**) and the difference was statistically significant ($p < 0.0001$) (**Fig. 2c**). In one representative experiment (Exp. 1), viral rebound was observed in cells treated with EFdA only, but not in cells treated with both EFdA and PEP005 (**Fig. 2d**). Viral rebound from EFdA + PEP005-treated cells was not detected (in the supernatant or intracellularly) even after stimulation with tumor necrosis factor-α (TNF-α) in week 17, confirming lack of replication-competent HIV-1 in the treated sample (**Fig. 2e and f**). Combinations with other antiretroviral agents, i.e., Darunavir (DRV, a protease inhibitor) and Dolutegravir (DTG, an integrase inhibitor), or other LRAs (SAHA, an HDAC inhibitor; prostratin, a PKC activator) were also tested (**Supplementary Fig. 2**). In general, antiretroviral drugs (DRV, DTG, and EFdA) effectively decreased supernatant HIV-1 levels, whereas most LRAs failed to suppress

viral replication when used on their own. However, the combination of an LRA with an antiretroviral drug delayed or inhibited viral recurrence after treatment was discontinued. Among several drug combinations analyzed in the present study, only the EFdA + PEP005 combination resulted in an experimental cure. Further drug screening may enable the identification of potent drug combinations to achieve experimental cure *in vitro*.

Prolonged drug treatment preferentially selects defective viruses in the *in vitro* model, mimicking the *in vivo* scenario. To elucidate the possible mechanism(s) underlying the experimental cure *in vitro,* we quantitatively and qualitatively analyzed HIV-1 proviruses from the model. We analyzed cell-associated HIV-1 DNA loads in one representative experiment (Exp. 6) (**Supplementary Fig. 3a**) and found that the HIV-1 DNA load was markedly decreased in samples treated with EFdA alone. The addition of PEP005 to EFdA further decreased the HIV-1 DNA load (**Fig. 3a**). After drug discontinuation, the HIV-1 DNA load increased in the sample treated with EFdA alone but not in the sample treated with both drugs (**Fig. 3a**). Accordingly, we characterized the structure of the HIV-1 proviral genome by nearly full-length PCR, using a single copy of the HIV-1 genome as a template[28]. We observed an increased proportion of a defective HIV-1 genome after EFdA treatment, possibly due to preferential elimination of intact, replication-competent proviruses (**Fig. 3b and c**). The tendency was more apparent upon a combined treatment with EFdA and PEP005 (**Fig. 3b and c**). All proviruses detected in the sample after a combined EFdA and PEP005 treatment were defective proviruses 17 weeks after initiation of drug treatment (**Fig. 3b and c**).

To compare the pattern of defective provirus accumulation *in vitro* and *in vivo*, peripheral blood samples of HIV-1-carrying individuals (**Supplementary Table 1**) were examined by nearly full-length, single-genome PCR. Before the initiation of cART, 25–42% proviruses in PBMCs from patients were defective, and the ratio increased to 83–100% after successful cART (treatment duration of at least 6 years) (**Fig. 3d** and **Supplementary Fig. 4**).

The data suggest an accumulation of defective proviruses *in vivo* caused by a preferential selection of defective and/or replication-incompetent proviruses during long-term antiretroviral treatment, in line with previous reports[21,28].

Furthermore, we observed a significant decrease in the HIV-1 DNA level induced by the EFdA and PEP005 combination in Exp. 6 (**Fig. 3e**), similar to that in Exp. 1 (**Fig. 2d**). However, nearly full-length HIV-1 PCR and sequencing analysis revealed that all provirus amplicons were full-length upon combination treatment (**Fig. 3f)**, with no critical mutations or deletions in the regions coding for viral proteins. However, these cells did not transcribe HIV-1 mRNA after TNF-α stimulation (**Supplementary Fig. 3b**). Some regions of 5′LTR and 3′LTR are not amplified by nearly full-length HIV-1 PCR[28]. Therefore, we explored the possibility of deletions or mutations in the provirus outside the primer-binding sites of nearly full-length HIV-1 PCR. We first determined HIV-1 ISs by LM-PCR, as previously described[24], and found that one infected clone was remarkably expanded (**Fig. 3g**). Part of the 5′LTR, including the transcription start site, in the expanded clone was deleted (**Fig. 3h** and **Supplementary Fig. 3c**). This may explain the observed lack of virus rebound. In another experiment in which no HIV-1 rebound was observed (**Supplementary Fig. 5a and b**), we identified a 1-bp deletion that generated a stop codon in the HIV-1 provirus *gag* sequence (**Supplementary Fig. 5c and d**). These observations indicate that a combination of EFdA and PEP005 enhances the elimination of intact and replication-competent HIV-1 proviruses, selected only for replication-incompetent proviruses, and thus achieved an experimental cure.

We further observed the following underlying mechanisms for replication incompetence: (1) large deletion(s) in viral protein-coding regions; (2) critical mutation(s), such as nonsense mutations and frame-shift mutations, in the viral coding sequence; and (3) abnormalities in HIV-1 proviral transcription (a schematic diagram is shown in **Supplementary Fig. 6**)[28-30]. We termed this new *in vitro* selection and elimination assay "the widely distributed intact provirus elimination (WIPE) assay." As shown in **Fig. 3d** and **Supplementary Fig. 4**,

long-term antiretroviral treatment also reduced the numbers of replication-incompetent proviruses and increased the proportion of defective HIV-1 proviruses *in vivo*. However, it is likely that a minor cell population with "replication-competent" HIV-1 proviruses persists during the long period of cART, maintaining the ability to reverse HIV-1 latency[9,21]. In the WIPE assay, the addition of an LRA seemed to accelerate the elimination of cells infected with replication-competent HIV-1 proviruses that exist as a minor population in Jurkat/NL cells.

Experimental cure achieved in the new *in vitro* model is associated with reactivation of latent HIV-1 reservoirs. The rationale behind using LRA as an HIV-1 cure is reactivating the latent HIV-1 provirus and inducing cell apoptosis via cytopathic effects or recognition by the host antiviral immunity[4,7,11,12,31]. We therefore investigated whether the experimental cure observed in the present study was indeed mediated by the reactivation of latent reservoirs.

First, we investigated the presence of latent clones in the Jurkat/NL system by infecting Jurkat-LTR-green fluorescent protein (GFP) cells (Jurkat cells stably transfected with a plasmid containing the GFP reporter gene driven by the HIV-1 promoter LTR) with HIV-1_{NL4-3}. In this system, Tat expression was monitored by GFP expression. We sorted and stimulated the GFP-negative cell fraction with TNF-α and found that the treatment increased proviral transcription in this fraction (**Fig. 4a,b**), indicating the presence of latent reservoirs in the Jurkat/NL system. The percentage of such reservoir cells was determined to be approximately 1% (**Fig. 4c**). Since antiviral cytotoxic T-lymphocytes (CTLs) and antibodies are absent in the Jurkat/NL system, latent HIV-1-infected cells reactivated by PEP005 would have been eliminated mainly by viral cytopathicity or cell apoptosis (**Supplementary Fig. 1c**)[10-12]. Therefore, we examined intracellular p24 levels and cell apoptosis during the early phase of drug treatment and observed an increase in p24 protein expression in cells treated with PEP005 (+/− EFdA) just 6 h after drug treatment initiation (**Fig. 4d**), which was followed by an increase in annexin V expression (**Fig. 4e**). The number of intracellular $p24^+$ cells decreased in EFdA- or

EFdA + PEP005-treated cell populations, and these cells constituted less than 2.5% of the total population by week 2 (**Fig. 4f**). On week 4, we analyzed caspase-3 levels in these cells and found that caspase-3 expression was much higher in $p24^+$ cells, especially in the EFdA + PEP005-treated cells, than in $p24^-$ cells (**Fig. 4g**). These observations suggest that PEP005 functions as an LRA, inducing apoptosis in cells latently infected with HIV-1 and facilitating an HIV-1 cure *in vitro*.

Next, we analyzed the effect of PEP005 on the widely distributed HIV-1 proviruses in the host cellular genome[20,21]. Copy numbers of intracellular HIV-1 DNA was markedly decreased after EFdA- or EFdA + PEP005-treatment (**Fig. 3d,** week 3). The proportion of the full-length-type provirus among total proviruses in EFdA alone or EFdA + PEP005-treated cells was also decreased but was nonetheless more than 50% after the initial 3-week treatment (**Fig. 4h**), suggesting that more than half of all proviruses were replication-competent at this time point. Collectively, these data indicate that the experimental cure achieved in this study was at least partially due to the reactivation of latent HIV-1 reservoirs in the WIPE assay.

Genetic and epigenetic environment of the HIV-1 provirus impacts its drug susceptibility in the novel *in vitro* model. We next investigated whether the drug susceptibility of various clones depends on the genetic and epigenetic environments of the HIV-1 provirus[32]. The proportion of ISs in the host genes was slightly decreased in EFdA- or EFdA + PEP005-treated cells (**Fig. 5a**). Changes in the epigenetic features of HIV-1 ISs during the initial phase of drug treatment were also apparent (**Fig. 5b**). EFdA treatment decreased the proportion of ISs with histone modifications, such as H3K27ac (indicative of open chromatin) and H3K36me3 (present in actively transcribed gene bodies). Theoretically, cells harboring HIV-1 proviruses in an open chromatin region with H3K27ac and/or H3K36me3 modifications would be prone to the production of viral particles and have a reduced half-life because of viral cytopathic effects (**Fig. 5c**). This seems to the case in the WIPE assay, because we observed that the EFdA or

EFdA + PEP005 treatment was more effective in reducing HIV-1 proviruses residing in the open chromatin regions than those in closed regions (**Fig. 5d**). HIV-1 proviruses lacking H3K27ac or H3K36me3 modifications were less susceptible to EFdA or EFdA + PEP005 treatment than those with H3K27ac or H3K36me3 modifications; however, the addition of PEP005 reduced the absolute proviral DNA load both with and without these histone modifications compared with that of EFdA treatment alone (**Fig. 5d**). Collectively, these findings indicate that the epigenetic environment of integrated proviruses plays a role in determining susceptibility during the "shock and kill" strategy, providing a mechanistic insight into the specific factors of HIV-1-infected clones that contribute to LRA susceptibility.

DISCUSSION

A number of studies have demonstrated that recently developed small-molecule compounds have the ability to reverse latently HIV-1 infected cells[5-8]. The usage of LRAs aims to reactivate latent proviruses and induce production of HIV-1 virions or viral antigens. The host human DNA does not exist in its naked form but possesses histone proteins and forms a chromatin structure. Integrated HIV-1 proviral DNA is also under the same regulation as the human genome. Proviral transcription is controlled by a combination of host cellular transcription factors that drive HIV-1 LTR promoter and accessibility of the transcription factors to the HIV-1 LTR. The epigenetic environment of the provirus plays a role in determining accessibility of transcription factors to the 5′LTR (**Fig. 5c**). In addition, HIV-1 preferentially integrates into gene bodies with active transcription, resulting in a high proportion of HIV-1 integration within the host gene body[33] (**Fig. 1f**). Transcriptional interference between the host genes and integrated proviruses is another factor that affects proviral transcription[34,35]. In line with this notion, a recent study reported that there is a higher proportion of intact proviruses integrated in the opposite orientation relative to the host genes in $CD4^+$ T cells of HIV-1-infected individuals[20]. These findings indicate that susceptibility to LRAs among

different HIV-1 clones is variable depending on the genetic and epigenetic environments of integrated proviruses. However, the *in vitro* latent models currently available for drug screening carry only one or two integrated HIV-1 proviruses with specific genetic and epigenetic patterns (**Fig. 1d**). Thus, a compound can potently reactivate a specific HIV-1 provirus in a latent cell line but may not do so for other clones. To our knowledge, there is no *in vitro* model available for evaluating the effect of LRAs on a variety of HIV-1 clones at present. Thus, we established a new *in vitro* assay, termed WIPE, for evaluating HIV-1 persistence and latency and which harbors a thousand different clones with a similar distribution of HIV-1 proviruses as observed *in vivo* (**Fig. 1e** and **f**).

We utilized the WIPE assay to evaluate the reduction and eradication of replication competent HIV-1-DNA after a combination therapy of existing ART drug(s) with LRA(s). In the Jurkat/NL system, there is a continuous and dynamic viral infection, including *de novo* infection, cell apoptosis triggered by viral production, replication of uninfected cells, and generation of latently infected cells. ART drugs inhibit *de novo* infection from infected to uninfected cells, while LRAs activate latently infected cells and induce reactivation of viral antigen expression. As there are no antiviral CTLs and antibodies in the WIPE assay, elimination of reactivated cells is mostly due to viral cytopathicity or apoptosis of the reactivated cells. Notably, we recently reported that some LRAs, such as PEP005, strongly induce the upregulation of active caspase-3, resulting in enhanced apoptosis[12,36]. Thus, the addition of an LRA appeared to successfully accelerate the elimination of latently HIV-1-infected cells in the WIPE assay.

We further characterized the HIV-1 provirus during the WIPE assay and found that the epigenetic environment of the provirus plays a role in drug susceptibility (**Fig 5b–e**) by analyzing the relationship between the HIV-1 provirus and histone modifications associated with open chromatin regions (H3K27Ac and HeK36me3); however, other factors may also contribute to drug susceptibility. Utilizing the WIPE assay along with an in-depth

characterization of the HIV-1 provirus would provide further insights on the underlying mechanism of HIV-1 latency, which cannot be obtained using conventional latent cell lines. Further studies using the WIPE assay may also provide mechanistic insights on molecular targeting, not only by LRAs but also by novel strategies; for example, the "block-and-lock" strategy was recently proposed, in which particular agents lock the HIV-1 promoter in a deep latency state to prevent viral reactivation[37,38].

The drug treatment with PEP005 and EFdA had a significant effect on the distribution of proviruses after only 3 weeks of treatment (**Fig 5d** and **e**), suggesting that we can evaluate LRAs without completing the full WIPE assay, which normally takes more than 15 weeks. This would increase the throughput of the WIPE assay as an *in vitro* screening model for LRA. Moreover, the WIPE assay is more similar to the situation *in vivo* than are conventional latent cell lines for HIV-1 in terms of heterogeneity of virus-infected clones. Nevertheless, compared with the WIPE assay host cells (the T cell line Jurkat), host cells *in vivo* are much more heterogenous. Recently, Battivelli et al.[32] reported that all tested LRAs could reactivate no more than 5% of cells with latent proviruses using their primary $CD4^+$ T cell model, suggesting that there is a wide variation in drug susceptibility to LRAs among different HIV-1-infected clones. Heterogeneity of the host $CD4^+$ T cells would also contribute to different drug susceptibility. Therefore, we propose the use of the WIPE assay to evaluate candidate LRA drugs for initial evaluation. Then, compounds with potent activity in the WIPE assay can be further evaluated by long-term drug assays using primary $CD4^+$ T cell-derived HIV-1 latent reservoir models[39] or animal models (i.e., HIV-1-infected humanized mice or SIV-infected macaques). This strategy may facilitate an increase in the efficiency of drug development for LRAs and help identify potent LRAs to reduce the reservoir size *in vivo*.

In this study, we used a Jurkat/NL system, which is a T cell-derived cell line (Jurkat) that possess the X4 HIV-1 variant. However, analyzing HIV-1-latency in monocytes or macrophages with the R5 HIV-1 variant is also very important. Thus, we obtained PM1CCR5

cells infected with R5-tropic HIV-1_{JRFL} (PM1CCR5/JRFL) but failed to maintain long-term chronic infection to evaluate drug efficacy (data not shown). For future research, cell culture models with R5 HIV-1 infected, monocyte-derived cells would be important for analyzing the differences in the latency mechanisms between the X4 HIV-1 and R5 HIV-1 variants.

Taken together, our findings provide a proof-of-concept for the "shock and kill" strategy against HIV-1 infection using our newly established *in vitro* assay. A combination of the persistent and heterogeneous HIV-1 infection *in vitro* model and high-throughput characterization of HIV-1 proviruses will be useful in developing a new generation of LRAs specific for HIV-1 proviral latency and for optimizing drug combinations to reduce the HIV-1 reservoir in an effort to achieve an HIV cure.

METHODS

Drugs and reagents. The anti-HIV-1 reverse-transcriptase inhibitor EFdA/MK-8591/ISL[26] and the protease inhibitor DRV[40] were synthesized, as previously described. PEP005 (PKC activator) was purchased from Cayman Chemical (Ann Arbor, MI); SAHA (vorinostat; HDAC inhibitor) from Santa Cruz Biotechnology (Dallas, TX); JQ-1 (BRD4 inhibitor) from BioVision (Milpitas, CA); GSK525762A (BRD4 inhibitor) from ChemScene (Monmouth Junction, NJ); Ro5-3335 from Merck (Darmstadt, Germany); and Al-10-49 (CBFβ/RUNX inhibitor) from Selleck (Houston, TX). Prostratin and Bryostatin-1 (PKC activator) were purchased from Sigma-Aldrich (St. Louis, MO), while Panobinostat (HDAC inhibitor), GS-9620 (TLR-7 agonist), and Birinapant (IAP inhibitor) were purchased from MedChem Express (Monmouth Junction, NJ). Phorbole 12-myristate13-acetate (PMA) and TNF-α were purchased from Wako Pure Chemical (Osaka, Japan) and BioLegend (San Diego, CA), respectively.

Establishment of the HIV-1 chronically infected cell culture model. Various T cell-derived cell lines [Jurkat, MT-4, Hut78, Molt4 (ATCC), Jurkat-LTR-GFP (JLTRG), and PM1-CCR5

(NIH AIDS Reagent Program)] were used to obtain cell populations with chronic HIV-1 infection. Cells were infected with HIV-1_{NL4-3} or HIV-1_{JRFL} (PM1-CCR5) and cultured in RPMI 1640 medium (Sigma-Aldrich) supplemented with 10% fetal calf serum (Sigma-Aldrich), 50 U/mL penicillin, and 50 μg/mL kanamycin. Cells were passaged weekly to maintain cell numbers < 5×10^6 cells/mL when confluent. p24 levels in the supernatant were monitored using Lumipulse G1200 (FUJIREBIO, Tokyo, Japan). The number of cells with intracellular p24 was also monitored on day 30 after infection by flow cytometry (as described below).

HIV-1 reversal in latently infected cells and caspase-3 activation by LRAs. Chronically HIV-1_{NL4-3}-infected Jurkat/NL cells were treated with 1 of the 11 drugs (1 μM) for 24 h, after which changes in supernatant p24 levels and induction of caspase-3 activation were determined by flow cytometry.

Flow cytometry analysis. The ratios of intracellular HIV-1 $p24^+$ cells, GFP^+ cells, and the active form of caspase-3 expression were determined as previously described[9,12,36]. Briefly, Jurkat/NL or JLTRG/NL cells were washed twice with phosphate buffered salts (PBS) and stained with Ghost Dye Red 780 (TONBO Biosciences, San Diego, CA) for 30 min at 4°C. The cells were then fixed with 1% paraformaldehyde/PBS for 20 min, and permeabilized in a flow cytometry perm buffer (TONBO Biosciences). After 5-min incubation at room temperature (25–30°C), cells were stained with anti-HIV-1 p24 (24-4)-fluorescein isothiocyanate (FITC) monoclonal antibody (mAb; Santa Cruz Biotechnology) and/or Alexafluor 647-conjugated anti-active caspase-3 mAb (C92-605; BD Pharmingen, San Diego, CA) for 30 min on ice. For propidium iodide (PI)/annexin V staining, cells were washed twice with PBS and resuspended in annexin V binding buffer (BioLegend) at a concentration of 1×10^7 cells/mL. The cells were then stained with FITC annexin V (BioLegend) and PI solution (BioLegend) for 15 min at room temperature. Cells were analyzed using a BD FACSVerse flow cytometer (BD Biosciences,

Franklin Lakes, NJ). Data collected were analyzed using FlowJo software (Tree Star, Inc., Ashland, OR).

Sorting of GFP^+ or GFP^- cells from HIV-1_{NL4-3}-infected JLTRG cells. HIV-infected Jurkat-LTR-GFP cells (6×10^6) were resuspended in FACS buffer (PBS with 1% fetal calf serum), after which GFP^+ or GFP^- cells were sorted using BD FACS Aria I (BD Biosciences). The sorted GFP^- cells were stimulated with 10 ng/mL TNF-α for 6 h and then GFP expression levels were analyzed using BD FACSVerse (BD Biosciences). The level of *gag* expression after 18-h stimulation with 10 ng/mL TNF-α was analyzed by reverse-transcription (RT)-digital droplet PCR (ddPCR). ddPCR droplets were generated using the QX200 droplet generator (Bio-Rad Laboratories, Hercules, CA). RT-PCR was performed using a C1000 Touch thermal cycler (Bio-Rad Laboratories) with the primers listed in **Supplementary Table 2**. The *gag*-positive and negative droplets were quantified based on fluorescence using the QX200 droplet reader (Bio-Rad Laboratories).

Determination of antiviral activity of LRAs and conventional anti-HIV-1 drugs in Jurkat/NL cells (WIPE assay). Jurkat/NL cells (5.0×10^4 cells/ml) were treated with a drug (e.g., EFdA, DRV, or PEP005) or a combination of drugs in a 12-well plate. Culture medium was exchanged and the drug was added. Drug treatment was stopped approximately on week 9 and the culture was maintained for an additional 8 weeks without drug supplementation. Supernatant p24 levels and intracellular HIV-1-DNA levels were monitored weekly during cell culture. At the end of each experiment, drug-treated cells with low/undetectable supernatant p24 levels were stimulated with 10 ng/mL TNF-α to confirm viral recurrence.

Isolation of PBMCs from patients with HIV-1. The study was performed in accordance with the guidelines of the Declaration of Helsinki. Analysis of clinical samples shown in **Fig. 1e** was

399 conducted based on a protocol reviewed and approved by the Kumamoto University
400 (Kumamoto, Japan) Institutional Review Board (approval number Genome 258).
401 Peripheral blood samples analyzed as shown in **Supplementary Fig. 4** were
402 collected from patients infected with HIV-1 before or after receiving cART for at least 7 years.
403 The Ethics Committee of the National Center for Global Health and Medicine (Tokyo, Japan)
404 approved this study (NCGM-G-002259-00). Informed written consent was obtained from all
405 patients (**Supplementary Table 1**) prior to the study. All subjects maintained low viral loads (<
406 20 copies/mL; except for occasional blips) during therapy. $CD4^+$ T-cell counts in peripheral
407 blood samples ranged from 447 to 632 cells/mm^3 (average 529 cells/ mm^3). The plasma viral
408 loads were < 20 copies/mL, as determined by quantitative PCR (Roche COBAS
409 AmpliPrep/COBAS TaqMan HIV-1 Test version 2.0) at the time of enrollment in the study.
410 PBMCs were isolated from whole blood by density-gradient centrifugation using
411 Ficoll-Paque™ (GE Healthcare, Chicago, IL). Total cellular DNA was extracted and used in
412 subsequent PCR experiments.

413

414 **Quantification of intracellular HIV-1 DNA levels.** Total cellular DNA was extracted from
415 cells (cell lines or PBMCs) using a QIAmp DNA Blood mini kit (Qiagen, Hilden, Germany)
416 according to manufacturer's instructions. Quantitative PCR (qPCR) analysis of intracellular
417 HIV-1 DNA levels was conducted using Premix Ex Taq (Probe qPCR) Rox plus (Takara Bio,
418 Kusatsu, Japan). The oligonucleotides HIV-1 LTR and β2-microglobulin were used for HIV-1
419 DNA quantification and cell number determination, respectively (primer sequences are provided
420 in **Supplementary Table 2**[41-44]). HIV-1 proviral DNA copy and cell numbers were calculated
421 based on a standard curve generated using a serially diluted pNL4-3 plasmid and DNA
422 extracted from Jurkat cells, respectively.

423

424 **RT-qPCR for HIV-1 mRNA quantification.** Total cellular RNA was extracted from Jurkat

cells infected with HIV-1 using the RNeasy Mini Kit (Qiagen) according to manufacturer's instructions. cDNA was synthesized using the PrimeScript RT Master Mix (Takara Bio). RT-qPCR analysis of intracellular HIV-1 RNA was performed using PowerUp SYBR Green Master Mix (Applied Biosystems, Foster City, CA). Primer sequences used for the detection of HIV-1-RNA and β-actin gene are listed in **Supplementary Table 2**. To determine the reactivation of HIV-1 in Jurkat/NL cells, relative HIV-1-RNA expression levels were normalized to that of β-actin gene.

Amplification of near full-length single HIV-1 genome and sequencing. Nearly full-length single HIV-1 genome PCR was performed as described previously[28] with minor modifications. Briefly, genomic DNA was diluted to the single-genome level based on ddPCR and Poisson distribution statistics. The resulting single genome was amplified using Takara Ex Taq hot start version (first-round amplification). PCR conditions for first-round amplification consisted of 95°C for 2 min; followed by 5 cycles of 95°C for 10 s, 66°C for 10 s, and 68°C for 7 min; 5 cycles of 95°C for 10s, 63°C for 10 s, and 68°C for 7 min; 5 cycles of 95°C for 10 s, 61°C for 10 s, and 68°C for 7 min; 15 cycles of 95°C for 10 s, 58°C for 10 s, and 68°C for 7 min; and finally, 68°C for 5 min. First-round PCR products were diluted 1:50 in PCR-grade water and 5 μL of the diluted mixture was subjected to second-round amplification. PCR conditions for the second-round amplification were as follows, 95°C for 2 min; followed by 8 cycles of 95°C for 10 s, 68°C for 10 s, and 68°C for 7 min; 12 cycles of 95°C for 10 s, 65°C for 10 s, and 68°C for 7 min; and finally, 68°C for 5 min. Primer information is provided in **Supplementary Table 2**. PCR products were then visualized by electrophoresis on a 1% agarose gel. Based on Poisson distribution, samples with ≤ 30% positive reactions were considered to contain a single HIV-1 genome and were selected for sequencing. Amplified PCR products of the selected samples were purified using a QIAquick PCR Purification Kit (Qiagen) according to manufacturer's instructions. Purified PCR products were sheared by sonication using a Picoruptor device

(Diagenode, Liege, Belgium) to obtain fragments with an average size of 300–400 bp. Libraries for next-generation sequencing (NGS) were prepared using the NEBNext Ultra II DNA Library Prep Kit for Illumina (New England Biolabs, Ipwich, MA) according to manufacturer's instructions. Concentration of library DNA was determined using the Qubit dsDNA High Sensitivity Assay kit (Invitrogen, Carlsbad, CA). The libraries were subsequently pooled together, followed by quantification using the Agilent 2200 TapeStation and quantitative PCR (GenNext NGS Library Quantification kit; Toyobo, Osaka, Japan), and sequenced using the Illumina MiSeq platform (Illumina, San Diego, CA). The resulting short reads were cleaned using an in-house Perl script (kindly provided by Dr. Michi Miura, Imperial College London, UK), which extracts reads with a high index-read sequencing quality (Phred score > 20) in each position of an 8-bp index read. Next, adapter sequences from Read1 and Read2 were removed, followed by a cleaning step to remove reads that were too short or had a very low Phred score, as previously described[24]. The clean sequencing reads were aligned with the NL4-3 reference genome (GenBank-M19921) using the BWA-MEM algorithm[45]. Further data processing and cleanup, including the removal of reads with multiple alignments and duplicated reads, were performed using Samtools[45] and Picard (http://broadinstitute.github.io/picard/). The aligned reads were visualized using Integrative Genomics Viewer[46], and consensus sequences were copied and aligned using MUSCLE[47]. NGS analyses of nearly full-length HIV-1 PCR products from PBMCs of HIV-1-infected individuals were conducted using MinION platform with Flow Cell R9.4.1 and Rapid Barcoding kit (Oxford Nanopore Technologies, Oxford, UK), according to manufacturer's instructions. Sequencing reads cleaned using EPI2ME software (Oxford Nanopore Technologies) were aligned and analyzed as described above.

Ligation-mediated PCR (LM-PCR). Detection of HIV-1 ISs was performed using ligation-mediated PCR and high-throughput sequencing, as previously described[24] but with minor modifications. Briefly, cellular genomic DNA was sheared by sonication using the

Picoruptor device to obtain fragments with an average size of 300–400 bp. DNA ends were repaired using the NEBNext Ultra II End Repair Kit (New England Biolabs) and a DNA linker[24] was added. The junction between the 3′LTR of HIV-1 and host genomic DNA was amplified using a primer targeting the 3′LTR and a primer targeting the linker[24]. PCR amplicons were purified using the QIAquick PCR Purification Kit (Qiagen) according to manufacturer's instructions. This was followed by Ampure XP bead purification(Beckman Coulter). Purified PCR amplicons were quantified using Agilent 2200 TapeStation and quantitative PCR (GenNext NGS library quantification kit; Toyobo). LM-PCR libraries were sequenced using the Illumina MiSeq as paired-end reads, and the resulting FASTQ files were analyzed as previously described[24]. A circos plot showing virus ISs in the Jurkat/NL4-3 model and different cell lines was constructed using the OmicCircos tool available as a package in R software[48].

Bioinformatic analysis. Bed files containing the IS information were generated from the analyzed exported files. Data on RefSeq genes were obtained using UCSC Genome Browser (https://genome.ucsc.edu/) and the positions of RefSeq genes were compared with those of IS using the R package hiAnnotator (http://github.com/malnirav/hiAnnotator). Histone modifications of primary helper memory T cells from peripheral blood were obtained from ChIP-Seq datasets from the ENCODE project[49]. The relationship between HIV-1 ISs and histone modifications was analyzed as previously described[24].

Statistical analysis. Differences between groups were analyzed for statistical significance using the Mann-Whitney U test and log-rank test. Data were analyzed using a chi-squared test with Prism 7 software (GraphPad Software, Inc., La Jolla, CA), unless otherwise stated. Statistical significance was defined as $P < 0.05$.

REFERENCES

1. Finzi, D. *et al.* Identification of a reservoir for HIV-1 in patients on highly active antiretroviral therapy. *Science* **278**, 1295–1300 (1997).
2. Siliciano, J. D. *et al.* Long-term follow-up studies confirm the stability of the latent reservoir for HIV-1 in resting CD4+ T cells. *Nat. Med.* **9**, 727–728 (2003).
3. Chun, T. W., Davey, R. T., Jr., Engel, D., Lane, H. C. & Fauci, A. S. Re-emergence of HIV after stopping therapy. *Nature* **401**, 874–875 (1999).
4. Richman, D. D. *et al.* The challenge of finding a cure for HIV infection. *Science* **323**, 1304-1307 (2009).
5. Laird, G. M. *et al.* Ex vivo analysis identifies effective HIV-1 latency-reversing drug combinations. *J. Clin. Invest.* **125**, 1901–1912 (2015).
6. Jiang, G. *et al.* Synergistic Reactivation of Latent HIV Expression by Ingenol-3-Angelate, PEP005, Targeted NF-kB Signaling in Combination with JQ1 Induced p-TEFb Activation. *PLoS Pathog.* **11**, e1005066 (2015).
7. Bullen, C. K., Laird, G. M., Durand, C. M., Siliciano, J. D. & Siliciano, R. F. New ex vivo approaches distinguish effective and ineffective single agents for reversing HIV-1 latency in vivo. *Nat. Med.* **20**, 425–429 (2014).
8. Cillo, A. R. *et al.* Quantification of HIV-1 latency reversal in resting CD4+ T cells from patients on suppressive antiretroviral therapy. *Proc. Natl. Acad. Sci. U. S. A.* **111**, 7078–7083 (2014).
9. Matsuda, K. *et al.* Benzolactam-related compounds promote apoptosis of HIV-infected human cells via protein kinase C-induced HIV latency reversal. *J. Biol. Chem.* **294**, 116–129 (2019).
10. Kim, Y., Anderson, J. L. & Lewin, S. R. Getting the "Kill" into "Shock and Kill": Strategies to Eliminate Latent HIV. *Cell Host Microbe* **23**, 14–26 (2018).
11. Badley, A. D., Sainski, A., Wightman, F. & Lewin, S. R. Altering cell death pathways as an approach to cure HIV infection. *Cell Death Dis.* **4**, e718 (2013).
12. Hattori, S. I. *et al.* Combination of a Latency-Reversing Agent With a Smac Mimetic Minimizes Secondary HIV-1 Infection in vitro. *Front. Microbiol.* **9**, 2022 (2018).
13. Søgaard, O. S. *et al.* The Depsipeptide Romidepsin Reverses HIV-1 Latency In Vivo. *PLoS Pathog.* **11**, e1005142 (2015).
14. Rasmussen, T. A. *et al.* Panobinostat, a histone deacetylase inhibitor, for latent-virus reactivation in HIV-infected patients on suppressive antiretroviral therapy: a phase 1/2, single group, clinical trial. *Lancet HIV* **1**, e13–21 (2014).

15. Elliott, J. H. *et al.* Short-term administration of disulfiram for reversal of latent HIV infection: a phase 2 dose-escalation study. *Lancet HIV* **2**, e520–529 (2015).

16. Archin, N. M. *et al.* Administration of vorinostat disrupts HIV-1 latency in patients on antiretroviral therapy. *Nature* **487**, 482–485 (2012).

17. Maldarelli, F. *et al.* HIV latency. Specific HIV integration sites are linked to clonal expansion and persistence of infected cells. *Science* **345**, 179–183 (2014).

18. Wagner, T. A. *et al.* HIV latency. Proliferation of cells with HIV integrated into cancer genes contributes to persistent infection. *Science* **345**, 570–573 (2014).

19. Cohn, L. B. *et al.* HIV-1 integration landscape during latent and active infection. *Cell* **160**, 420–432 (2015).

20. Einkauf, K. B. *et al.* Intact HIV-1 proviruses accumulate at distinct chromosomal positions during prolonged antiretroviral therapy. *J. Clin. Invest.* **129**, 988–998 (2019).

21. Ho, Y. C. *et al.* Replication-competent noninduced proviruses in the latent reservoir increase barrier to HIV-1 cure. *Cell* **155**, 540–551 (2013).

22. Borducchi, E. N. *et al.* Antibody and TLR7 agonist delay viral rebound in SHIV-infected monkeys. *Nature* **563**, 360–364 (2018).

23. Gillet, N. A. *et al.* The host genomic environment of the provirus determines the abundance of HTLV-1-infected T-cell clones. *Blood* **117**, 3113–3122 (2011).

24. Satou, Y. *et al.* Dynamics and mechanisms of clonal expansion of HIV-1-infected cells in a humanized mouse model. *Sci. Rep.* **7**, 6913 (2017).

25. Symons, J. *et al.* HIV integration sites in latently infected cell lines: evidence of ongoing replication. *Retrovirology* **14**, 2 (2017).

26. Nakata, H. *et al.* Activity against human immunodeficiency virus type 1, intracellular metabolism, and effects on human DNA polymerases of 4'-ethynyl-2-fluoro-2'-deoxyadenosine. *Antimicrob. Agents Chemother.* **51**, 2701–2708 (2007).

27. Salie, Z. L. *et al.* Structural basis of HIV inhibition by translocation-defective RT inhibitor 4'-ethynyl-2-fluoro-2'-deoxyadenosine (EFdA). *Proc. Natl. Acad. Sci. U. S. A.* **113**, 9274–9279 (2016).

28. Imamichi, H. *et al.* Defective HIV-1 proviruses produce novel protein-coding RNA species in HIV-infected patients on combination antiretroviral therapy. *Proc. Natl. Acad. Sci. U. S. A.* **113**, 8783–8788 (2016).

29. Sanchez, G., Xu, X., Chermann, J. C. & Hirsch, I. Accumulation of defective viral

genomes in peripheral blood mononuclear cells of human immunodeficiency virus type 1-infected individuals. *J. Virol.* **71**, 2233–2240 (1997).

30. Bruner, K. M. *et al.* Defective proviruses rapidly accumulate during acute HIV-1 infection. *Nat. Med.* **22**, 1043–1049 (2016).

31. Abner, E. & Jordan, A. HIV "shock and kill" therapy: In need of revision. *Antiviral Res.* **166**, 19–34 (2019).

32. Battivelli, E. *et al.* Distinct chromatin functional states correlate with HIV latency reactivation in infected primary CD4(+) T cells. *Elife* **7**, e34655 (2018).

33. Schroder, A. R. *et al.* HIV-1 integration in the human genome favors active genes and local hotspots. *Cell* **110**, 521–529 (2002).

34. Han, Y. *et al.* Orientation-dependent regulation of integrated HIV-1 expression by host gene transcriptional readthrough. *Cell Host Microbe* **4**, 134–146 (2008).

35. Lenasi, T., Contreras, X. & Peterlin, B.M. Transcriptional interference antagonizes proviral gene expression to promote HIV latency. *Cell Host Microbe* **4**, 123–133 (2008).

36. Matsuda, K. *et al.* Inhibition of HIV-1 entry by the tricyclic coumarin GUT-70 through the modification of membrane fluidity. *Biochem. Biophys. Res. Commun.* **457**, 288–294 (2015).

37. Darcis, G., Van Driessche, B. & Van Lint, C. HIV Latency: Should We Shock or Lock? *Trends Immunol.* **38**, 217–228 (2017).

38. Kessing, C. F. *et al.* In Vivo Suppression of HIV Rebound by Didehydro-Cortistatin A, a "Block-and-Lock" Strategy for HIV-1 Treatment. *Cell Rep.* **21**, 600-611 (2017).

39. Saleh, S. *et al.* CCR7 ligands CCL19 and CCL21 increase permissiveness of resting memory CD4+ T cells to HIV-1 infection: a novel model of HIV-1 latency. *Blood* **110**, 4161–4164 (2007).

40. Koh, Y. *et al.* Novel bis-tetrahydrofuranylurethane-containing nonpeptidic protease inhibitor (PI) UIC-94017 (TMC114) with potent activity against multi-PI-resistant human immunodeficiency virus in vitro. *Antimicrob. Agents Chemother.* **47**, 3123–3129 (2003).

41. Butler, S. L., Hansen, M. S. & Bushman, F. D. A quantitative assay for HIV DNA integration in vivo. *Nat. Med.* **7**, 631–634 (2001).

42. Goff, L. K. *et al.* The use of real-time quantitative polymerase chain reaction and comparative genomic hybridization to identify amplification of the REL gene in

follicular lymphoma. *Br. J. Haematol.* **111**, 618–625 (2000).

43. Douek, D. C. *et al.* HIV preferentially infects HIV-specific CD4+ T cells. *Nature* **417**, 95–98 (2002).

44. Lee, G. Q. *et al.* Clonal expansion of genome-intact HIV-1 in functionally polarized Th1 CD4+ T cells. *J. Clin. Invest.* **127**, 2689–2696 (2017).

45. Li, H. & Durbin, R. Fast and accurate short read alignment with Burrows-Wheeler transform. *Bioinformatics* **25**, 1754–1760 (2009).

46. Robinson, J. T. *et al.* Integrative genomics viewer. *Nat. Biotechnol.* **29**, 24–26 (2011).

47. Edgar, R. C. MUSCLE: multiple sequence alignment with high accuracy and high throughput. *Nucleic Acids Res.* **32**, 1792–1797 (2004).

48. Hu, Y. *et al.* OmicCircos: A Simple-to-Use R Package for the Circular Visualization of Multidimensional Omics Data. *Cancer Inform.* **13**, 13–20 (2014).

49. EBCODE Project Consortium. An integrated encyclopedia of DNA elements in the human genome. *Nature* **489**, 57–74 (2012).

Acknowledgements

We thank Jumpei Ito for providing access to the Python program, allowing us to perform association analyses between the epigenetic environment and viral integration sites. This research was supported in part by grants from the Japan Agency for Medical Research and Development (grant numbers JP19fk0410015 to K.T., Y.S., and Ke.M.; JP19fk0410009 to Y.S.; JP19fk0410023 to K.T., P.M., and Y.S.; and JP19fk0410014 to Y.S.). Y.S. was also supported by grants from MEXT/JSPS KAKENHI (JP17890606) and JST MIRAI. K.T. and Ke.M. were also supported by a grant from the National Center for Global Health and Medicine, Japan (29a1010).

Author contributions

K.Y., Y.S., and Ke.M. designed the study. Ko.M., S.I., K.T., S.H., H.K., P.M., M.M., and N.S.D. performed the experiments. S.M. provided patient sample DNA. S.I., B.J.Y.T., and Y.S.

631 performed bioinformatic analysis. H.G., S.O., S.M., H.M., Y.S., and Ke.M. supervised the work.

632 Y.S. and Ke.M. wrote the manuscript with input from all authors.

633

634 **Competing interests**

635 The authors declare no competing financial or non-financial interests.

636

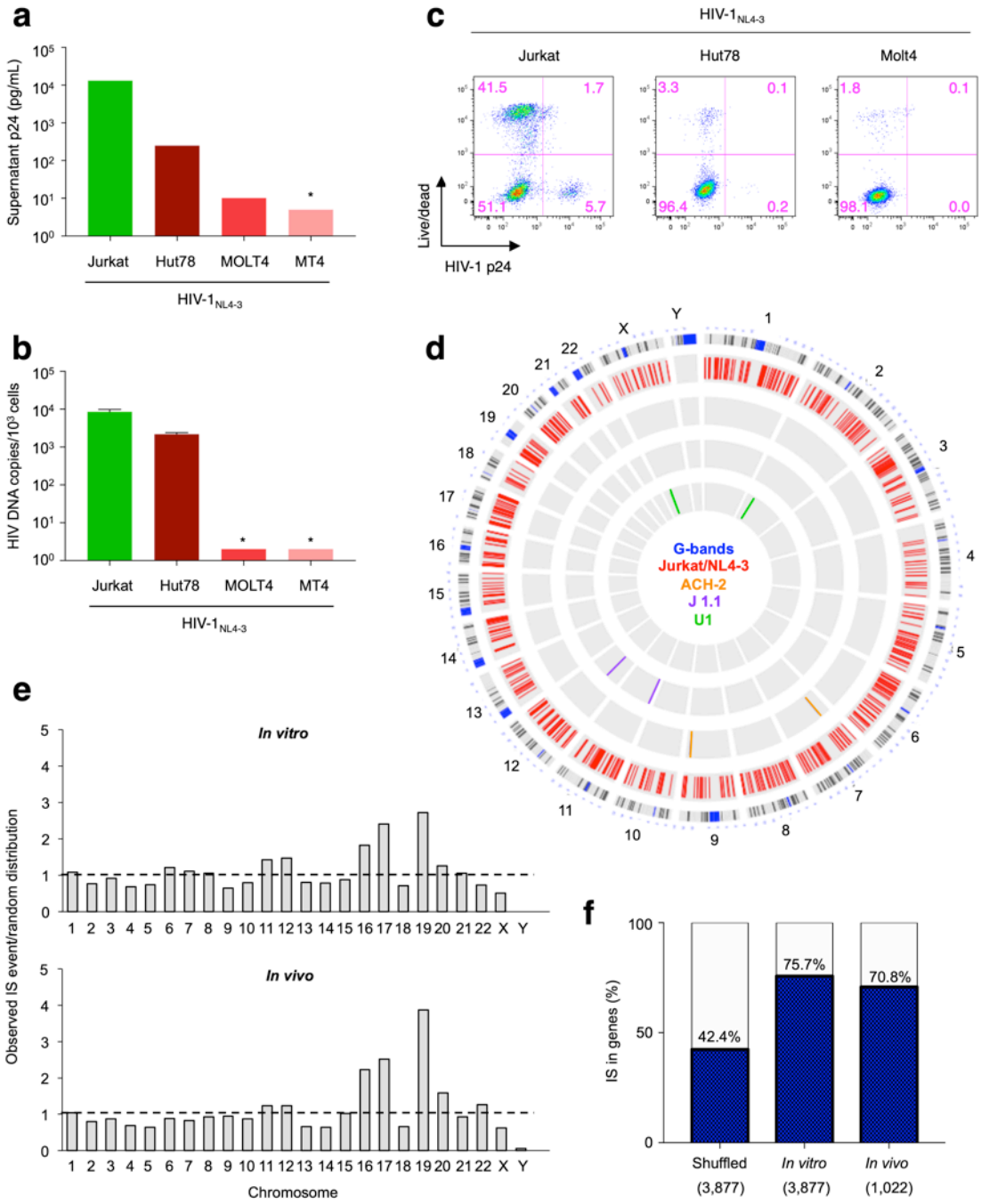

Fig. 1 | Establishment of a new *in vitro* HIV-1 infection model. To establish a cell culture model of long-term persistent HIV-1 infection, various T-cell lines (Jurkat, Hut78, MOLT4, and MT-4 cells) were used. HIV-1 production (**a**) and copies of intracellular HIV-1 DNA (**b**) on day 30 of each cell line **c,** Co-existence of p24-positive and p24-negative cell populations in HIV-1–infected Jurkat, Hut78, and MOLT4 cell lines. The percentage of intracellular p24-positive cells

was analyzed by flow cytometry. **d,** Circos plot depicting viral integration sites (IS) across the human genome in the Jurkat/NL system and in different cell lines *in vitro*. Each chromosome is presented on the outer circle and is broken down into sequential bins. Blue/black, red, orange, purple, and green bars indicate G-bands, Jurkat/NL system, ACH-2, J1.1, and U1, respectively. **e,** Comparison of HIV-1 IS frequency in the individual chromosomes in the *in vitro* model (Jurkat/NL) and *in vivo* in PBMCs from five HIV-1-infected individuals. The *y*-axis depicts the proportion of integration events observed relative to random distribution, with a horizontal dashed black line set at a value of 1. **f,** Relationship between HIV-1 IS and the host genes, *in vitro* and *in vivo*, compared via random distribution. Numbers in parentheses at the bottom of the bars indicate the numbers of unique ISs observed; numbers at the top of the bars indicate the percentage of HIV-1 proviruses integrated within the host genes in each group. Asterisk (*) stands for below detection limit.

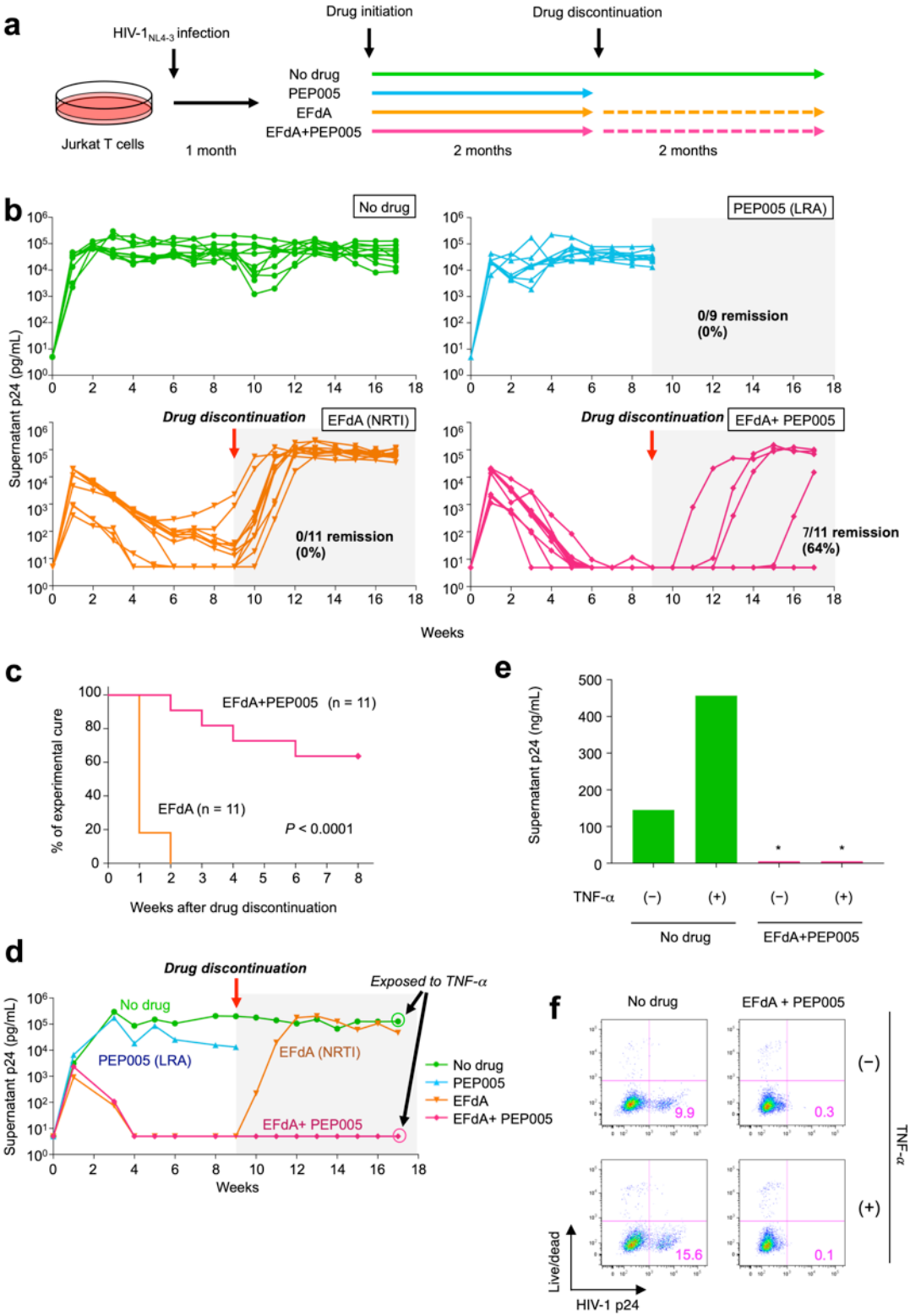

Fig. 2 | Effect of drug treatments on viral persistence in the new *in vitro* infection model. a, Assay overview. Schematic representation of the assay protocol involving the HIV-1_{NL4-3}–

infected cell culture model (Jurkat/NL cells). **b,** Changes in supernatant p24 levels without drugs, with 5 nM PEP005 or 50 nM EFdA, or with a combination of 50 nM EFdA and 5 nM PEP005 (n = 11, 9, 11, and 11, respectively). Drug treatment was terminated on week 9 but analysis continued for an additional 8 weeks. **c,** Log-rank test comparison of the percentage of non-recurrence in the EFdA single treatment and the combination treatment. **d,** Changes in supernatant p24 levels in a representative experiment (Exp. 1) from experiments shown in **Fig. 2b**. **e–f,** Assessment of the viral rebound in Jurkat/NL cells after drug discontinuation. Cells treated with drugs or untreated cells were stimulated with TNF-α (10 ng/mL) in week 17, and supernatant p24 (**e**) and intracellular p24 levels (**f**) were analyzed on day 6 after stimulation. Asterisk (*) denotes below detection limit.

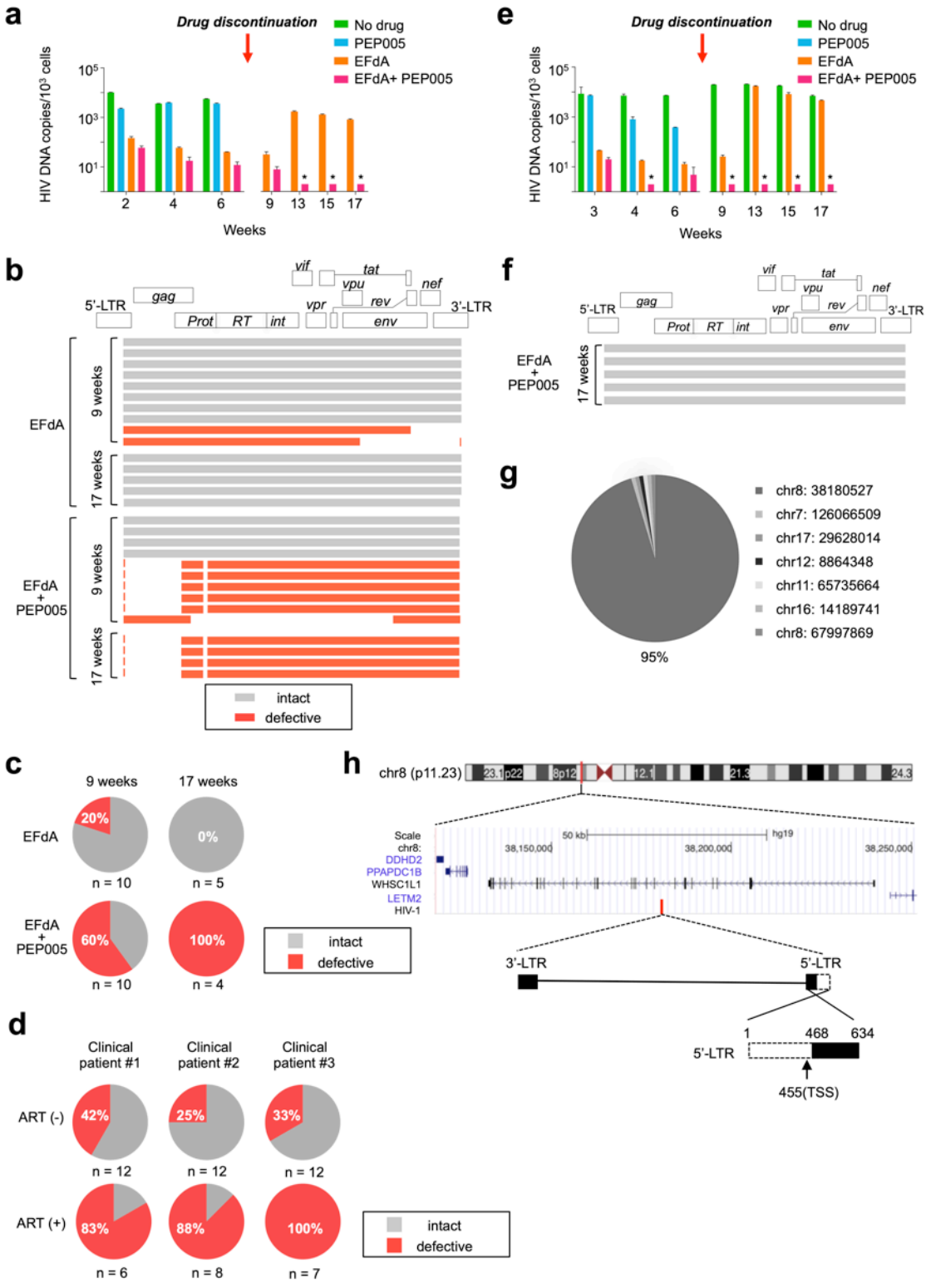

Fig. 3 | Mechanisms underlying experimental cure *in vitro*. a, Quantification of intracellular copies of HIV-1 DNA at each time point in Exp. 6 (**Supplementary Fig. 3a**). **b,** Schematic

representation of the individual provirus structures from two different treatment groups and at two time points in Exp. 6. Each horizontal bar represents an individual HIV-1 genome, as determined by amplification of near full-length HIV-1 DNA from a single HIV-1 genome and DNA sequencing. The gray bars denote full-length types and the red bars indicate defective proviruses. **c,** Pie charts reflecting the proportion of defective and intact proviruses in Exp. 6. **d**, Pie charts reflecting the proportion of defective and intact proviruses in PBMCs from three HIV-infected individuals. **e,** Quantification of intracellular copies of HIV-1 DNA at each time point in Exp. 1 (**Fig. 2d**). **f,** Schematic representation of the individual provirus structures in Exp. 1 for the EFdA/PEP005 culture group 17 weeks after drug treatment initiation. **g,** Pie chart showing the relative abundance of each HIV-1-infected clone. Chromosomal number and position of each clone is shown in the right panel. **h,** Schematic figure of the provirus structure and IS in the expanded clone. A 467-bp deletion in the 5′-end of 5′LTR was observed. TSS, transcription start site. Asterisk (*) stands for below detection limit.

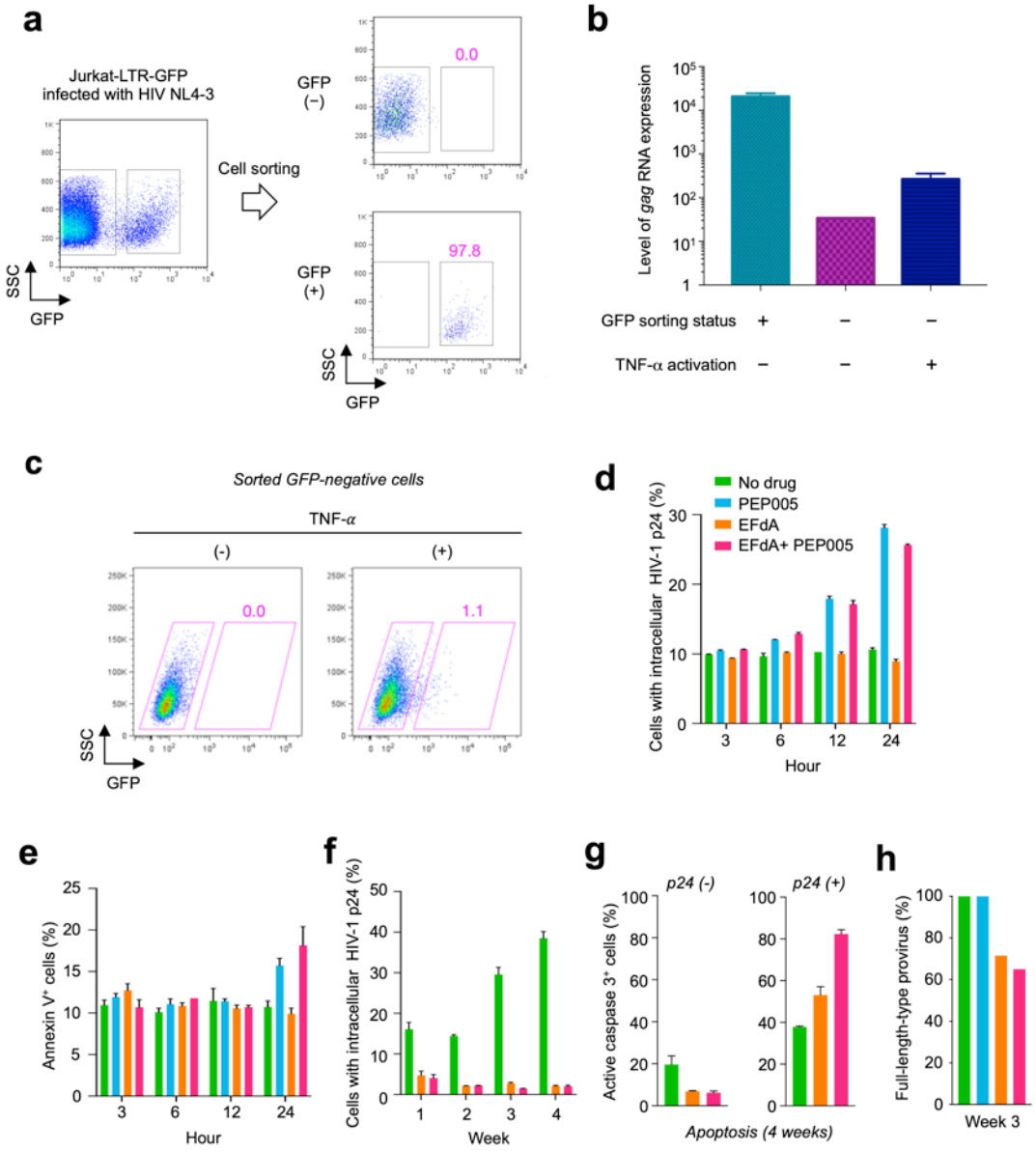

Fig. 4 | Proof-of-concept of the "shock and kill" strategy of the WIPE assay. a, Sorting of GFP-positive cells among HIV-1-infected Jurkat-LTR-GFP cells. GFP-positive (Tat^+) or GFP-negative populations (Tat^-) among HIV-1-infected Jurkat-LTR-GFP cells were sorted. **b,** GFP-negative cells were stimulated with 10 ng/mL TNF-α for 6 h and *gag* mRNA expression was quantified. **c**, GFP expression in sorted GFP-negative Jurkat-LTR-GFP cells infected with HIV-1_{NL4-3} was analyzed after 6 h of TNF-α stimulation (10 ng/mL). **d**–**e,** p24 expression and cell apoptosis during the early phase of drug treatment. Bar graphs show the change in the

percentage of cells expressing intracellular HIV-1 p24 (**d**) and annexin V (**e**) during the initial 24 h of drug treatment. **f,** Changes in the numbers of cells with intracellular p24 (weeks 1–4). **g,** Percentages of active caspase-3-positive cells in the p24-positive or p24-negative cell population. **h,** Percentages of full-length-type HIV-1 provirus after 3 weeks of drug treatment. Data represent the mean ± S.D. of three independent experiments.

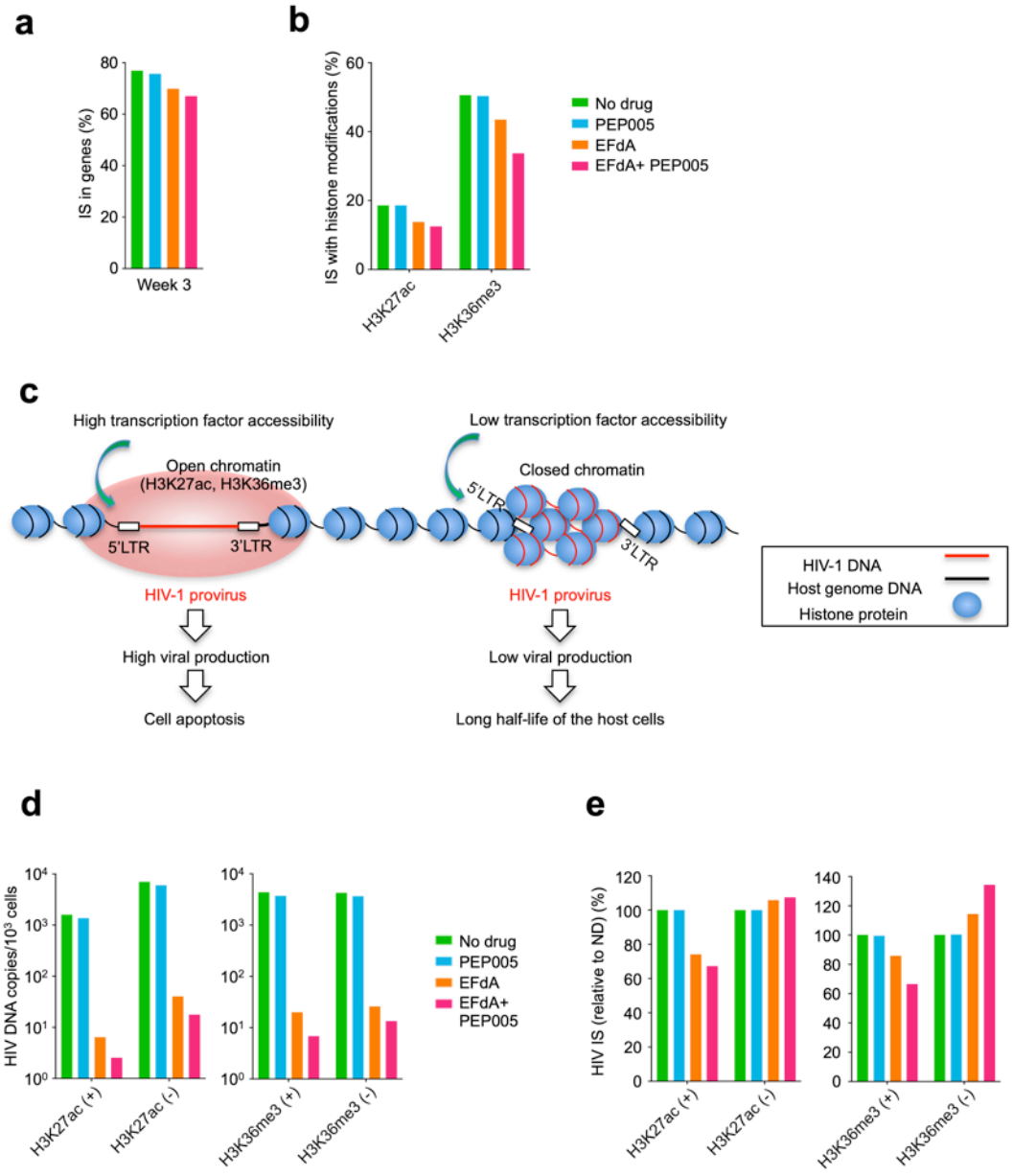

Fig. 5 | Factors affecting drug susceptibility in the WIPE assay. a, Percentages of HIV-1 proviruses integrated within the host genes. **b,** Percentages of HIV-1 ISs with histone modifications after 3 weeks of drug treatment. Histone modifications in primary helper memory T cells from peripheral blood were obtained from ChIP-Seq datasets from the ENCODE project[49]. **c,** Schematic figure showing different LRA susceptibility mediated by epigenetic status of the HIV-1 provirus. **d,** HIV DNA copies per 10^3 cells with or without the histone marks H3K27ac or H3K36me3 after 3 weeks of the initial drug treatment.

Extended Data Figures and Tables

The WIPE assay for selection and elimination of HIV-1 provirus *in vitro* using latency-reversing agents

Matsuda et al.

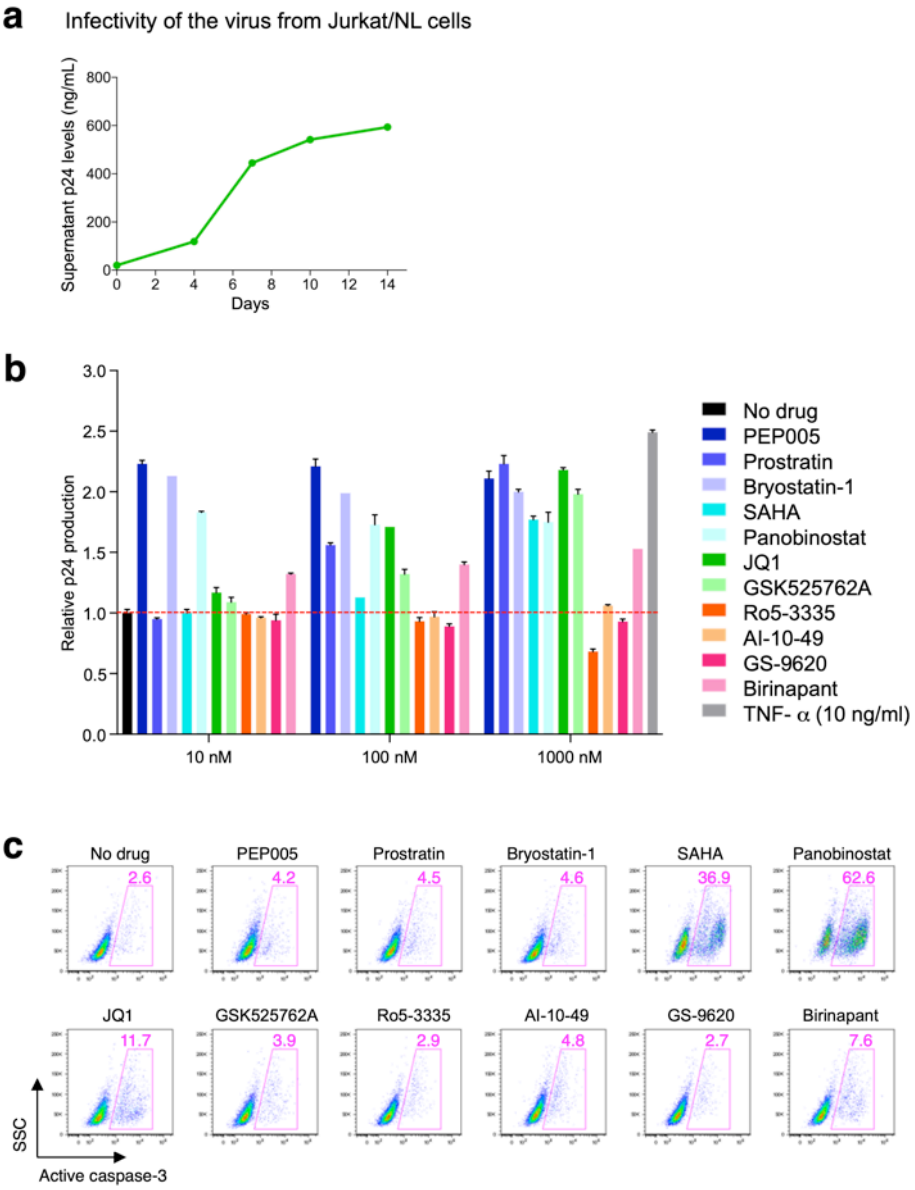

Extended Data Fig. 1 | Viral infectivity in Jurkat/NL cells and effects of LRAs on HIV-1 production and cell apoptosis. a, Infectivity of HIV-1_{NL4-3} produced from Jurkat/NL cells. MT4 cells were infected with the virus, cultured, and then supernatant p24 levels were measured. **b–c,** Efficacy of LRAs in inducing HIV-1 production or caspase-3 activation in Jurkat/NL cells. Cells were treated with a drug (1 μM) for 24 h and the changes in supernatant p24 values (**b**) or percentage of active forms of caspase-3 expression (**c**) were examined.

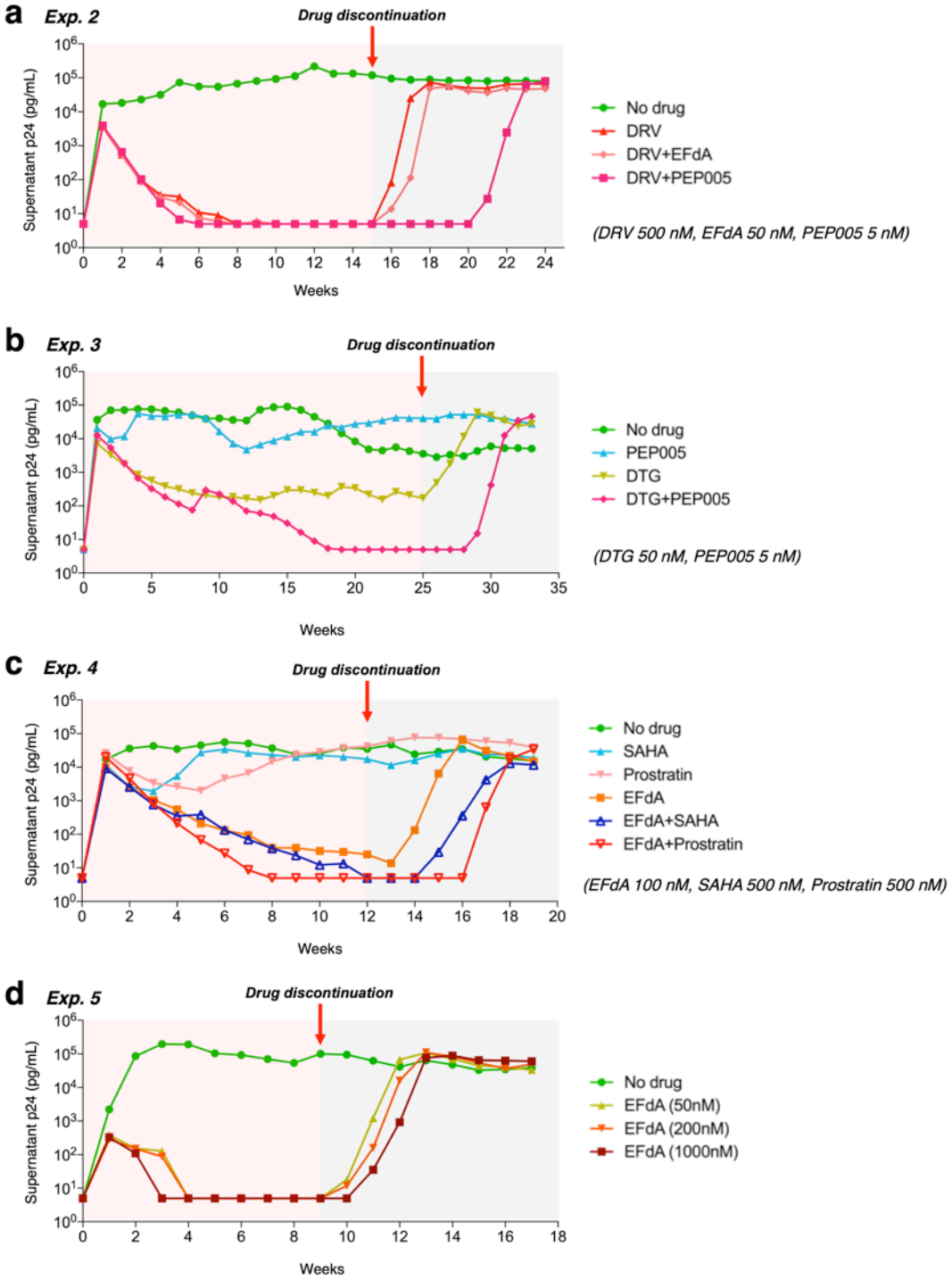

Extended Data Fig. 2 | Effect of various combinations of antiretroviral drugs and LRAs on viral persistence. Changes in HIV-1 production under treatment with 5 nM PEP005, 50 nM EFdA, and/or 500 nM Darunavir (DRV, protease inhibitor) (**a**), 5 nM PEP005, and/or 50 nM Dolutegravir (DTG, integrase inhibitor) (**b**), and 100 nM EFdA, 500 nM SAHA (HDAC inhibitor), and/or 500 nM prostratin (PKC activator) (**c**). **d,** EFdA at different concentrations (50 nM, 200 nM, and 1 μM) was examined. A higher concentration of EFdA (200 nM and 1 μM) slightly delayed the recurrence of supernatant viruses after treatment interruption.

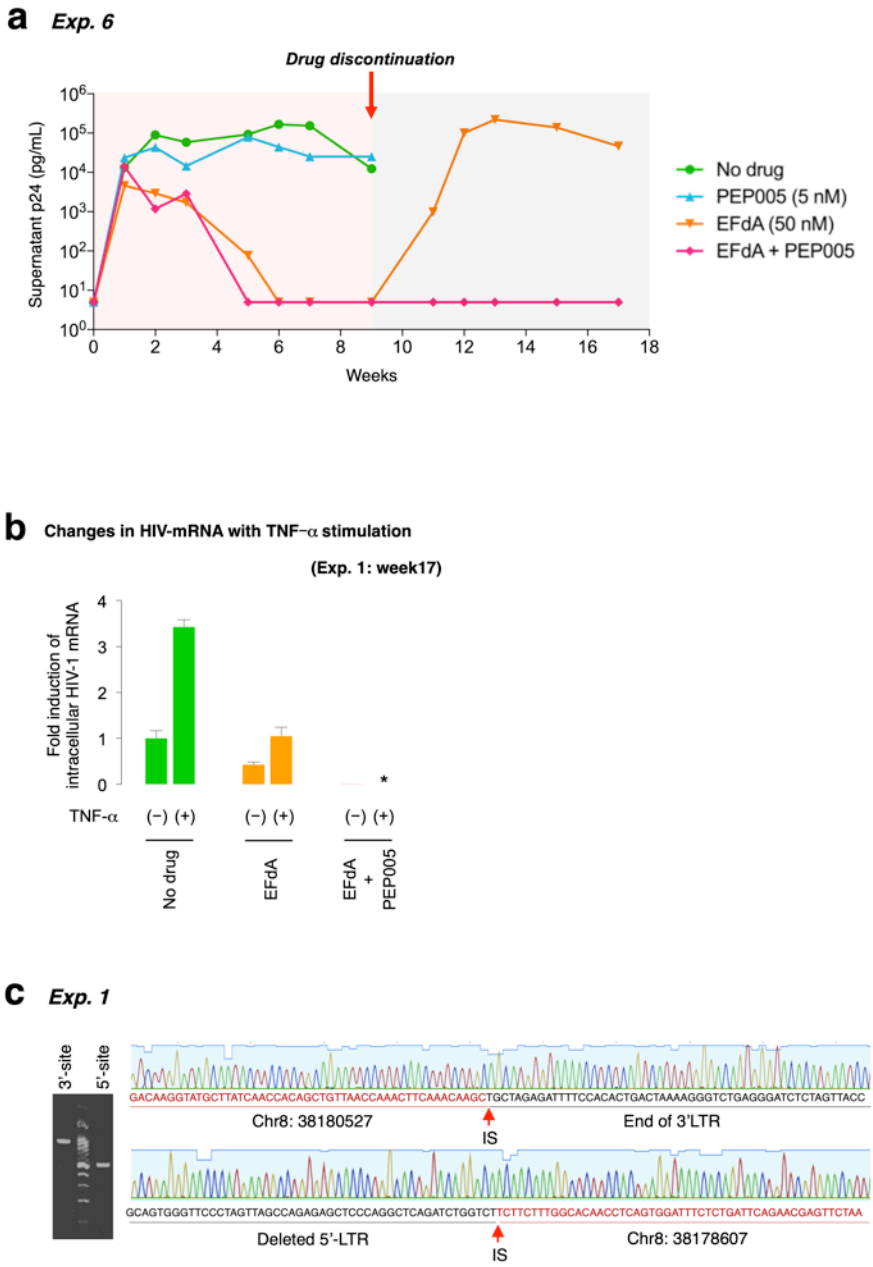

Extended Data Fig. 3 | Underlying mechanisms of the experimental cure (Exp. 1 and 6). a, Result of WIPE assay with EFdA and PEP005 in Exp. 6 (an experiment shown in **Fig. 2b**). **b**, Analysis of HIV-1 mRNA transcripts in cells of Exp. 1 (**Fig. 2d**) on week 17 with TNF-α stimulation. Cells were treated with 10 ng/mL TNF-α for 24 h, and the change in intracellular HIV-1-mRNA transcripts was analyzed. **c,** Result of IS-specific PCR of the expanded clone in Exp. 1 (**Fig. 3f**). PCR bands amplified from either 5′LTR- or 3′LTR-host junctions (502 bp and 773 bp, respectively) are shown on the left. DNA sequencing results of the host-virus junctions are shown on the right.

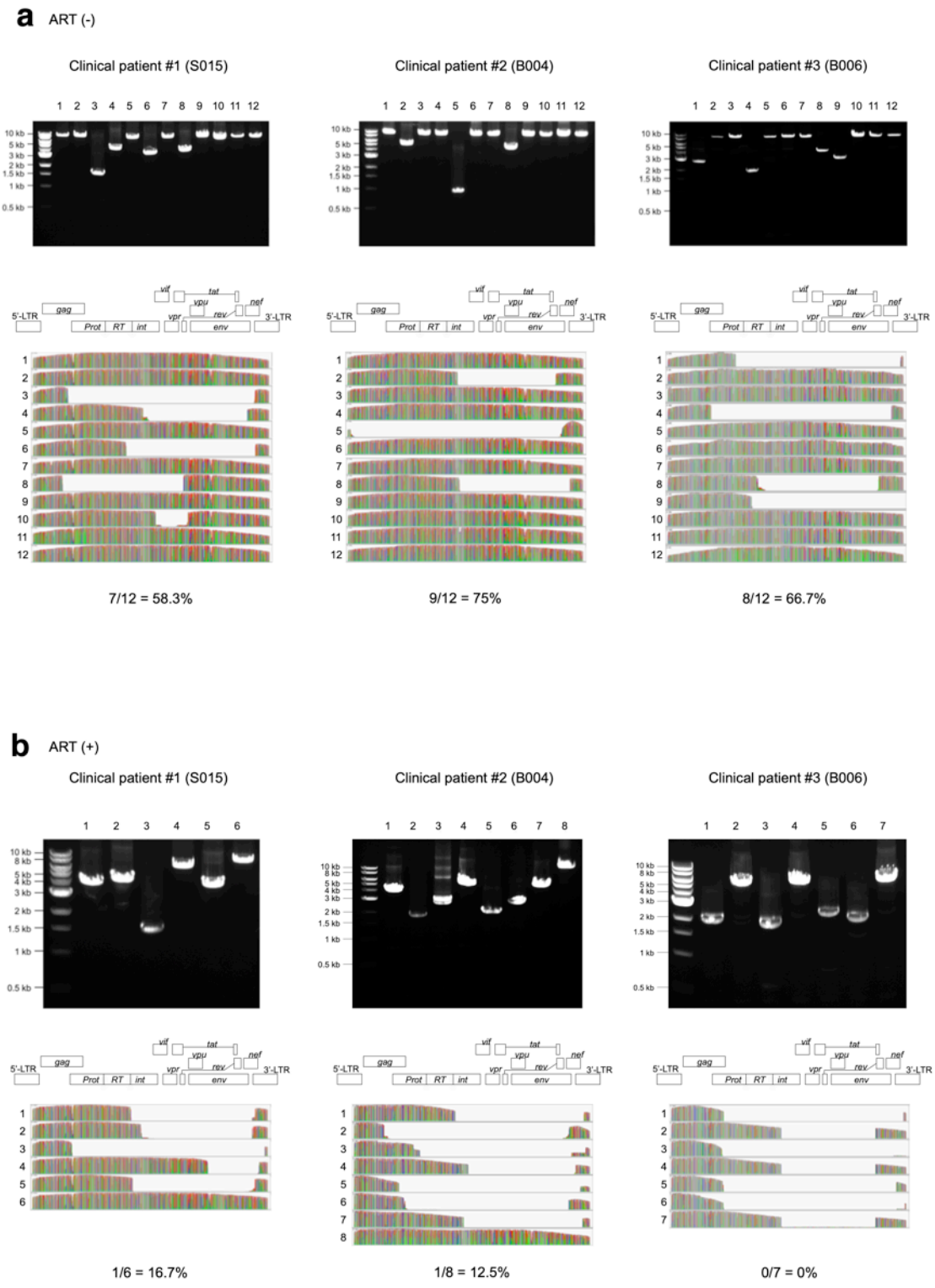

Extended Data Fig. 4 | Nearly full-length, single-genome PCR analysis of the primary cells of HIV-1 infected patients. a, PCR products of cells from three HIV-1 patients (**Extended Data Table 2**) before initiation of effective cART treatment. **b**, PCR products of cells from the same patients after cART treatment (duration, 84–264 months).

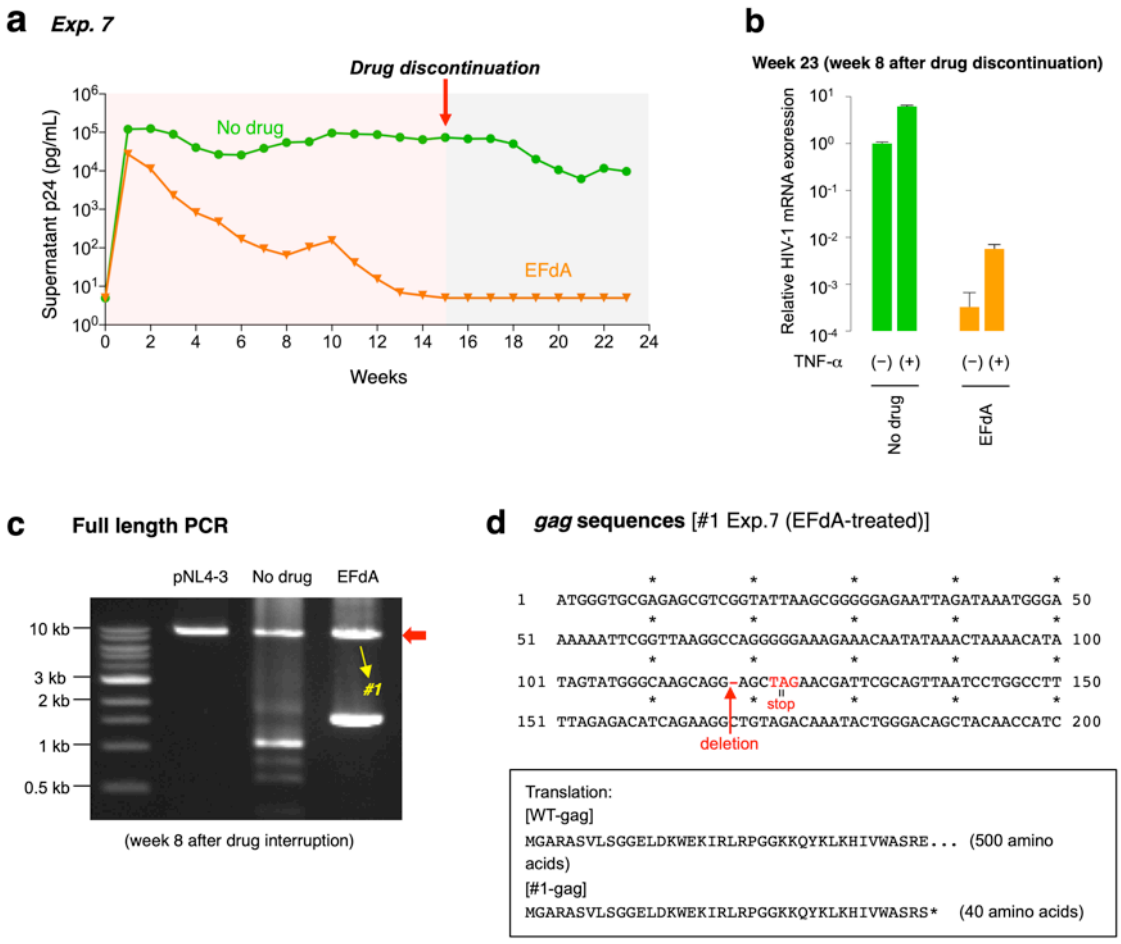

Extended Data Fig. 5 | An underlying mechanism of an experimental cure (Exp. 7). a, Treatment of Jurkat/NL cells with EFdA (Exp. 7). In this experiment, HIV-1 rebound was not observed in cells treated with EFdA until week 23; however, EFdA-treated cells showed an increase in HIV-1 mRNA expression with TNF-α stimulation (**b**), suggesting that the cells containing replication-competent proviruses are a minor population. **c,** PCR products (9031 bp) of cell samples from Exp. 7 on week 23. **d,** Sequencing analysis of PCR products (#1) in (**c**) with NGS demonstrated that there is a 1-bp deletion with a premature stop codon in HIV-1 *gag*.

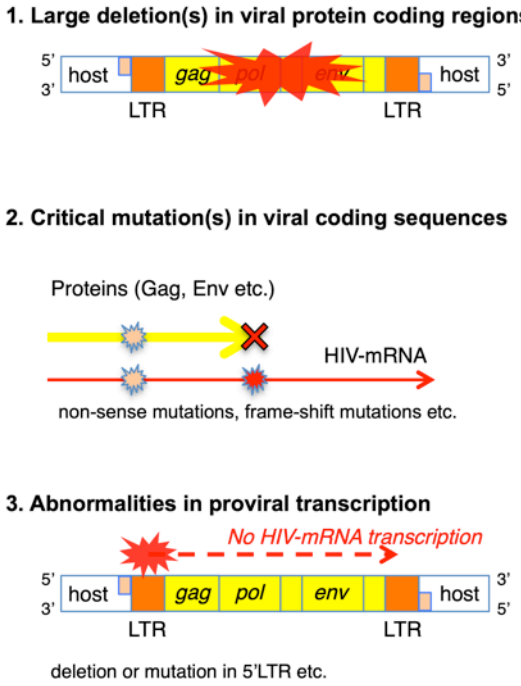

Extended Data Fig. 6 | Mechanism of HIV-1 provirus replication incompetency observed after drug treatment.

Extended Data Table 1. Characteristics of HIV-1-infected patients

Patient ID	M/F	Age	VL[a] (copies/mL)	CD4 count[a] (cells/mm^3)	cART	Therapy (years)	Plasma HIV RNA < 20 copies/mL for (years)
B-004	F	46	<20	447	FTC/TAF/EFV	19	7
B-006	M	56	<20	632	FTC/TAF/RPV	22	7
S-015	M	49	<20	509	FTC/TAF/COBI/EVG	7	6

[a]VL and CD4 count were measured at the time of the study.

COBI, cobicistat; EFV, efavirenz; EVG, elvitegravir; FTC, emtricitabine; RPV, rilpivirine; TAF, tenofovir alafenamide fumarate; VL, viral load.

Extended Data Table 2. PCR primers used in the present study

[Quantitative PCR]

Target	Primer name	Sequence (5′-3′)	Reference
HIV-1 LTR	MH531 (forward)	TGTGTGCCCGTCTGTTGTGT	34
	MH532 (reverse)	GAGTCCTGCGTCGAGAGAGC	34
	LRTp (probe)	FAM-CAGTGGCGCCCGAACAGGGA-BHQ1	34
β2-microglobulin	β2m_S (forward)	GGAATTGATTTGGGAGAGCATC	35
	β2m_AS (reverse)	CAGGTCCTGGCTCTACAATTTACTAA	35
	β2m_P (probe)	FAM-AGTGTGACTGGGCAGATCATCCACCTTC-BHQ1	35
HIV-1 gag	gag_S (forward)	GGTGCGAGAGCGTCGGTATTAAG	36
	gag _AS (reverse)	AGCTCCCTGCTTGCCCATA	36
β-actin	β-actin_S (forward)	GCGAGAAGATGACCCAGATC	11
	β-actin_AS (reverse)	CCAGTGGTACGGCCAGAGG	11

[Near full-length single HIV-1 genome PCR]

Primer set	Name	HXB2 position	Length (bp)	Sequence (5′-3′)	Reference
First round	DNA F1	623–649	9064	AAATCTCTAGCAGTGGCGCCCGAACAG-	27
	DNA R1	9652–9676		TGAGGGATCTCTAGTTACCAGAGTC	27
Second round	Nested F	638–666	8985	GCGCCCGAACAGGGACYTGAAARCGAAAG	37
	DNA R2	9603–9632		GCACTCAAGGCAAGCTTTATTGAGGCTTA	27

Second (clinical)	DNA F2	682–705	8951	TCTCTCGACGCAGGACTCGGCTTG	27
	DNA R2	9603–9632		GCACTCAAGGCAAGCTTTATTGAGGCTTA	27

[Linker-mediated PCR primers]

Target	Name	Sequence (5′-3′)	Reference
	Long linker	TCATATAATGGGACGATCACAAGCAGAAGACGGCATACG AGATNNNNNNNN CGGTCTCGGCATTC CTGCTGAACCGCTCTTCCGATCT	23
	Short linker	p-GA TCGGAAGAGCGAAAAAAAAAAAAA	23
1st PCR	B3	GCTTGCCTTGAGTGCTTCAAGTAGTGTG	23
	B4	TCATGATCAATGGGACGATCA	23
2nd PCR	P5B5	AATGATACGGCGACCACCGAGATCTACACGTGCCCGTCT GTTGTGTGACTCTGG	23
	P7	CAAGCAGAAGACGGCATACGAGAT	23

[High- throughput sequencing primers]

Target	Name	Sequence (5′-3′)	Reference
HIV-1	Read1	ATCCCTCAGACCCTTTTAGTCAGTGTGGAAAATCTC	23
Human genome	Read2	CGGTCTCGGCATTCCTGCTGAACCGCTCTTCCGATCT	23
Adaptor barcode	Index1	GATCGGAAGAGCGGTTCAGCAGGAATGCCGAGACCG	23